MITSUBISHI ELECTRIC RESEARCH LABORATORIES
http://www.merl.com

Locating Double-line-to-Ground Faults using Hybrid Current Profile Approach

Dubey, A.; Sun, H.; Nikovski, D.N.; Tomihiro, T.; Kojima, Y.; Tetsufumi, O.

TR2015-003 January 2015

Abstract

This paper proposes a hybrid current profile based fault location algorithm for double-line-to-ground (DLG) faults in a distribution system. The method uses both short-circuit fault current profile (average of fault currents recorded for the faulted phases) and during-fault load current profile (corresponding to the un-faulted phase) to estimate an accurate fault location. The method is extended to include the effects of fault resistance in determining the fault location. Both fault current profiles and load current profiles are simulated for different values of fault resistances. The profiles are also extrapolated for those fault resistances corresponding to which the simulated profiles are not available. Numerical examples on a sample distribution feeder with multiple laterals and load taps are provided to validate the proposed algorithm for its robustness.

2015 IEEE PES Innovative Smart Grid Technologies Conference (ISGT)

Locating Double-line-to-ground Faults using Hybrid Current Profile Approach

Anamika Dubey
University of Texas
at Austin
Austin, TX 78712, USA

Hongbo Sun, Daniel Nikovski
Mitsubishi Electric Research
Laboratories
Cambridge, MA 02139, USA

Tomihiro Takano, Yasuhiro Kojima,
and Tetsufumi Ohno
Mitsubishi Electric Corporation
Hyogo 661-8661 Japan

Abstract—**This paper proposes a hybrid current profile based fault location algorithm for double-line-to-ground (DLG) faults in a distribution system. The method uses both short-circuit fault current profile (average of fault currents recorded for the faulted phases) and during-fault load current profile (corresponding to the un-faulted phase) to estimate an accurate fault location. The method is extended to include the effects of fault resistance in determining the fault location. Both fault current profiles and load current profiles are simulated for different values of fault resistances. The profiles are also extrapolated for those fault resistances corresponding to which the simulated profiles are not available. Numerical examples on a sample distribution feeder with multiple laterals and load taps are provided to validate the proposed algorithm for its robustness.**

***Index Terms*--** **Distribution system; fault location analysis; short-circuit fault**

I. Introduction

Self-healing is one of the important characteristics of the smart grid. When a fault occurs, the system is required to automatically restore service to as many customers as possible, and as quickly as possible. Automatic fault location analysis plays an important role for implementing self-healing in distribution systems.

Fault location analysis in distribution systems has been extensively studied by both electric power engineers and researchers. The fault location methods deployed in a radial distribution system so far are broadly categorized as impedance-based methods [1-2], traveling waves based methods [3-4], knowledge-based methods [5-6], and model based methods [7-8]. Although, impedance-based methods are most commonly implemented [1, 2], the simplified circuit models used by impedance-based algorithms may lead to significant errors in fault locations.

Nowadays, using advanced simulation software an accurate model of the actual distribution circuit can be simulated. Model-based methods use simulated circuit models to determine the fault location. Such approaches are very simple to implement and are relatively more accurate than impedance-based methods. This kind of method takes the exact distribution circuit model into consideration, then the errors caused due to heterogeneous lines, load taps and laterals can be avoided. In [7-8], a model-based approach using short-circuit current profile is proposed. The fault currents are pre-calculated at each section of the feeder using the simulated circuit and are compared against the measured fault current. Short-circuit current profile based approach is easy to implement and more accurate if simulated sufficiently, but it does have certain limitations. One of its limitations is that the algorithm may result in multiple possible fault locations, since the distribution circuits are mainly radial with many power flow paths along the feeders. In [8], an impedance based algorithm is also implemented along the short circuit profile algorithm to narrow down the possible locations. But just as pointed by the authors of [8], determining one fault location might not be possible in all cases even when both algorithms are used. Another problem that is inherent with short-circuit current profile approach is the effect of fault resistance. Since, fault resistance is not included in calculating short-circuit current profile, the errors due to fault resistance are inevitable.

In this paper, a novel hybrid current-profile approach is proposed to determine fault location in an event of DLG fault. The fault location is determined based on the fault conditions recorded at a switch upstream from the actual fault location. The proposed approach uses both short-circuit fault current profile for the faulted phases, and during-fault load current profile for the un-faulted phase to determine the actual fault location. The measured load current on the un-faulted phase during the fault is used to identify the correct fault location amongst multiple possible locations that determined using fault current profiles. To predict the location of a fault with fault resistance, both fault and load current profiles are developed with varied values of fault resistances and stored into database, and exact fault distance and location are determined by using stored current profiles corresponding to each simulated fault resistance. For a fault with a fault resistance that not stored in the database, a linear extrapolation of available profiles is used to produce correct current profiles for determining the fault location. The testing results on a sample distribution circuit are given to demonstrate the capability of the proposed approach to determine fault location with multiple power flow paths and fault resistances.

II. Proposed Hybrid Current Profile Approach

This paper proposes a hybrid load and fault current profile approach to determine the location of a DLG fault. The proposed approach is illustrated using the distribution circuit shown in Fig. 1.

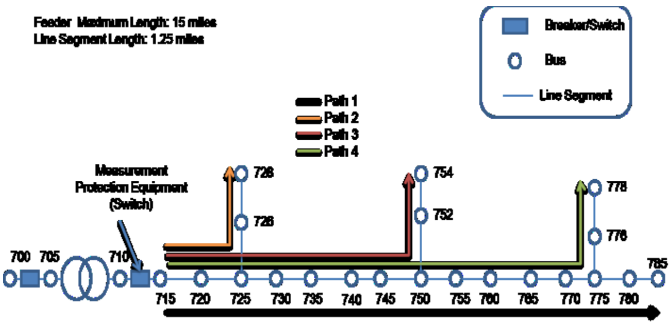

Figure 1. Simulated single-feeder test distribution circuit

The test system is an ungrounded single-feeder system. It includes 24 three-phase buses, and each bus has a three-phase DELTA-connected constant PQ load. Each line segment is a 1.25-mile long three-wire underground cable, and the maximum length of the feeder is 15 miles. Measurements corresponding to the fault are available at the switch present upstream from the feeder (i.e. bus 715). As shown in Fig. 1, the switch at bus 715 sees four power-flow paths.

A. Building Short-circuit Fault Current Profile and During-Fault Load Current Profile for Bolted DLG Faults

In order to estimate fault location more accurately and uniquely, both short circuit fault current profiles and during-fault load current profiles are developed for the feeder for a predetermined fault type, for example, a bolted DLG fault.

Given a distribution circuit model, the short-circuit fault current profile is developed by placing the DLG faults at successive incremental distances from the relay, and plotting the corresponding short-circuit fault currents against the distance to the fault. For the system in Fig. 1, the fault current profile is developed along each of the four paths by plotting an average of the fault currents recorded for the faulted phases. Fig. 2 gives the fault current profile for bolted DLG faults on the circuit of Fig. 1. Since the same type of cables are used for all line segments, the fault current profiles overlap for different power flow paths.

Figure 2. Short-circuit fault current profile for zero fault resistance

Similarly, a during-fault load current profile for the distribution circuit is developed by simulating a DLG fault at successive incremental distances along the distribution feeder, and plotting the during-fault load current corresponding to the un-faulted phase against the distance to fault. Similar to fault current profiles, load current profiles are also developed along each power flow path. Fig. 3 shows the load current profiles developed for the system shown in Fig. 1. It can be seen that the during-fault load currents corresponding to the un-faulted phase are significantly different along different power flow paths.

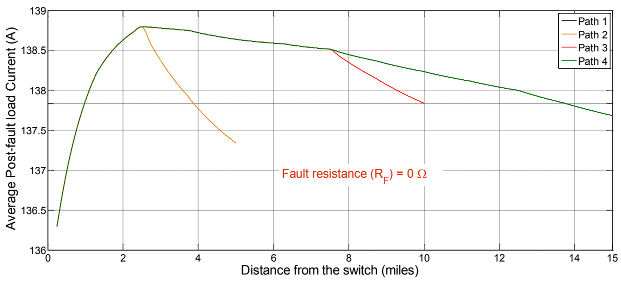

Figure 3. During-fault load current profile for zero fault resistance

On occurrence of a fault, the average fault current and during-fault load current are recorded. Both average fault current and during-fault load current are extrapolated on fault current profile and load current profile, respectively. Actual fault location is the common fault location identified by both current profiles.

B. Considering of the Effects of Fault Resistance

The magnitudes of fault currents are significantly affected by the fault resistance. In order to address the impacts of fault resistance, the current profiles are developed for different values of fault resistances.

Fig. 4 lists the fault current profiles for different values of fault resistances. In Fig. 4, fault resistance is varied to 0.5Ω, 1Ω, 2Ω, 4Ω, 6Ω, 8Ω, 10Ω, and fault current profiles are developed for each value of fault resistance. A DLG fault is simulated at successive incremental distances along the distribution circuit, and for each value of fault resistance average fault current is recorded. A plot is obtained for average fault current vs. distance to fault from the switch. Similar to the previous discussion, corresponding to a particular value of fault resistance, multiple subplots corresponding to multiple power-flow paths are obtained. Essentially the fault current profile consists of multiple exponentially decaying plots corresponding to each value of fault resistance, and each containing multiple subplots corresponding to multiple power-flow paths. Therefore if the effect of fault resistance is included in the fault current profile approach, for each value of fault resistance there could be a valid fault location.

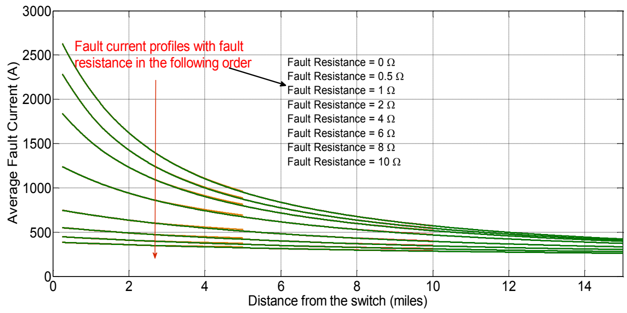

Figure 4. Short-circuit fault current profiles for varied fault resistances

To narrow down the fault location estimates, during-fault load current profiles are also developed. Similar to fault current profile, load current profiles are developed for each value of fault resistance. The current corresponding to un-faulted phase is recorded for each value of fault resistance, and a plot is obtained for during-fault load current vs. distance to fault from the switch. Clearly, for each fault resistance, load current profile consists of multiple subplots corresponding to multiple power-flow paths. Fig. 5 shows the load current profiles generated for different values of fault resistances.

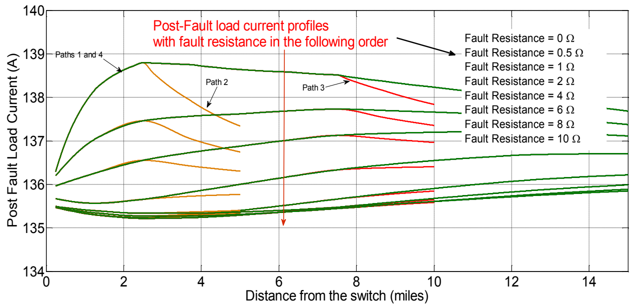

Figure 5. During-fault load current profiles for varied fault resistances

When a fault occurs, the average fault current and during-fault load current are recorded, and plotted on fault current and load current profiles. Corresponding to each fault resistance, location estimates are obtained using both fault current and load current profiles. Actual fault location is a common estimated location obtained from both current profiles for a particular value of fault resistance.

C. Extrapolating the Current Profiles for Intermediate Values of Fault Resistances

The method discussed in previous section might fail if the current profiles are not available in the database for the actual fault resistance corresponding to the test case. An approximate fault current and load current profiles are needed for an intermediate value of fault resistance.

Suppose that the test case corresponds to a 1.5 Ω fault resistance. Since the current profiles are not simulated for a fault resistance of 1.5 Ω, a match among location estimates obtained using fault and load current profiles will not be found within a reasonable tolerance. In that case, approximate current profiles are developed using a linear approximation of the current profiles corresponding to 1Ω and 2Ω fault resistances. To obtain a location estimate, the average fault current and during-fault load current are recorded and extrapolated on the approximate fault current profile and load current profile, respectively. Actual fault location is the fault location common to the results obtained from both current profiles for a particular value of fault resistance. The current profiles are approximated again if a location estimate is not obtained. The process is repeated till the location estimates obtained from both current profiles are within acceptable tolerance.

III. Determining Fault Location using Hybrid-Current Profile Approach

Both fault current profile and during-fault load current profile consists of multiple sub-profiles. Number of graphs further increases when the effect of fault resistance is included in the approach. Hence, when fault current magnitude is extrapolated, multiple location estimates would be obtained and hence it is essential to understand how the results should be interpreted. In this discussion the graphical interpretation of the results is presented. The proposed method is demonstrated using the distribution circuit shown in Fig. 1.

A. Case for Determing Location of a Bolted Fault

A bolted fault is simulated at bus 754 and the average fault current and during-fault load current is recorded. The average fault current is 572.5 A, and the during-fault load current recorded in un-faulted phase is 137.8 A. Fault location using fault current profile is obtained as shown in Fig. 6, and the fault is either 10 miles along path 1 or 10 miles along path 3. The fault location is confirmed to be 10 miles along path 3 when extrapolating the load current on load current profile, as illustrated in Fig. 7.

B. Case for Determining Location of a Fault with Fault Resistance for which Current Profiles are available in the Database

To illustrate this case, a DLG fault is simulated at bus 754, with fault resistance equal to 2 Ω. The average fault current recorded is 494 A.

The fault current is extrapolated on the fault current profiles corresponding to different fault resistances as shown in Fig. 8. The location estimates using the fault current profiles for each value of fault resistance are listed in Table I. The empty cells imply no intersection along that path for the corresponding value of fault resistance. Since the fault resistance is unknown, using only fault current profiles, estimated fault location can vary from 2.6 to 12.84 miles, and that covers almost entire feeder length.

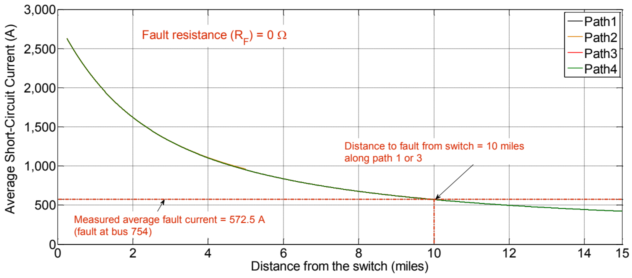

Figure 6. Estimating fault location of a bolted DLG fault using fault current profile

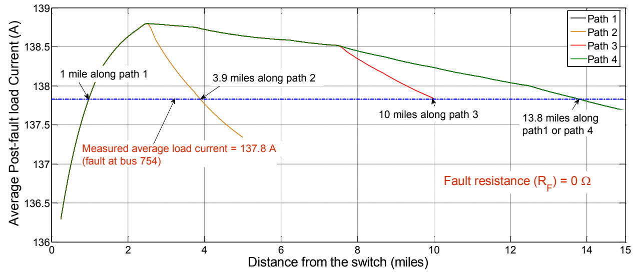

Figure 7. Estimating fault location of a bolted DLG fault using during-fault load current profile

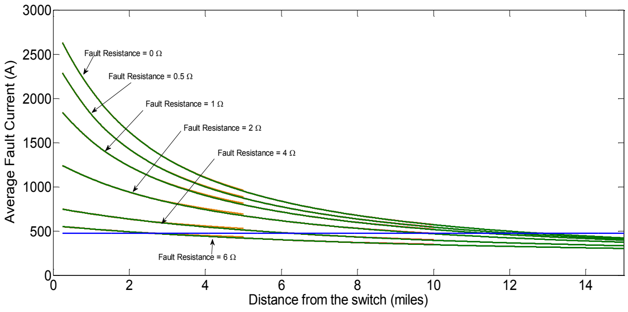

Figure 8. Location estimates using fault current profile when actual fault resistance is in the current database

TABLE I. Location Estimates using Fault Current Profile

Fault Resistance(Ω)	*Distance to fault along (miles)*			
	Path 1	**Path 2**	**Path 3**	**Path 4**
0	12.84			12.84
0.5	12.16			
1	11.42			
2	9.82		10	
4	6.3			
6	2.64	2.64		
8 and 10	No intersection			

To narrow down the location estimate to fewer possible values, load current profiles are used. The during-fault load current recorded for the test case is extrapolated on the load current profiles as shown in Fig. 9, and location estimates corresponding to each value of fault resistance are obtained and shown in Table II. The only location where estimated fault location calculated using both current profiles is approximately same is 10 miles along Path 3 for fault resistance equal to 2 Ω. Clearly, the estimated fault location matches to actual fault location.

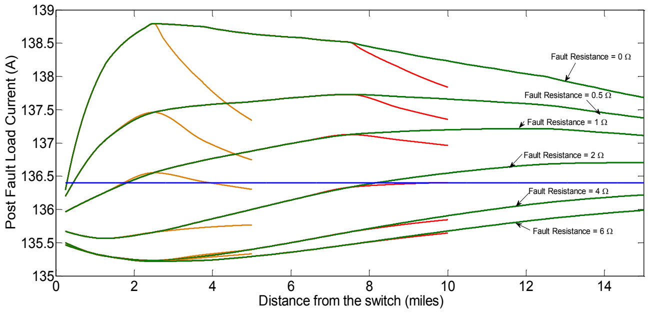

Figure 9. Location estimates using during-fault load current profile when actual fault resistance is in the current database

TABLE II. LOCATION ESTIMATES USING LOAD CURRENT PROFILE

Fault Resistance	*Distance to fault along (miles)*			
	Path 1	**Path 2**	**Path 3**	**Path 4**
0 Ω	0.29			
0.5 Ω	0.45			
1 Ω	1.82	2.51		
2 Ω	8.21		10	
4 Ω	15			15
6 Ω onwards	No intersection			

C. Case for Determining Location of a Fault with Fault Resistance for which Current Profiles are not available in the Database

In this case, the fault resistance is set as 1.5 Ω, and a DLG fault is simulated at bus 754. Again the actual fault location is 10 miles along path 3. The measured average fault current and during-fault load current are plotted on respective current profiles. Fig. 10-11 and Tables III-IV show the fault location estimates along various paths for different values of fault resistances.

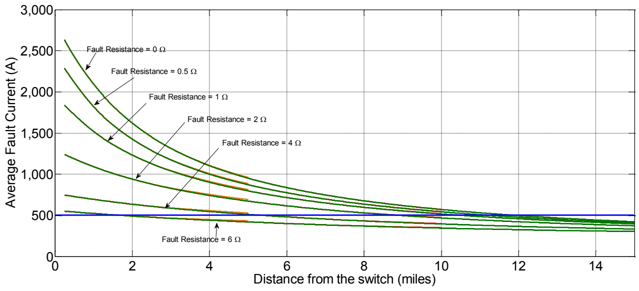

Figure 10. Location estimates using fault current profile when actual fault resistance is not in the current database

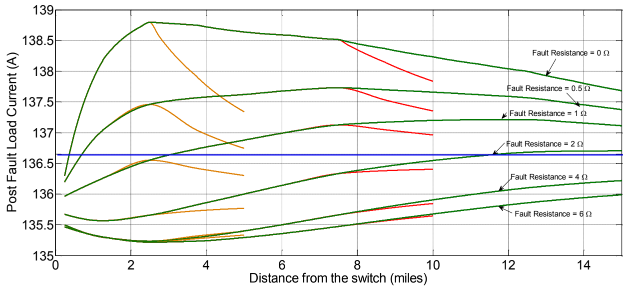

Figure 11. Location estimates using load current profile when actual fault resistance is not in the current database

TABLE III. LOCATION ESTIMATES USING FAULT CURRENT PROFILE

Fault Resistance(Ω)	*Distance to fault along (miles)*			
	Path 1	**Path 2**	**Path 3**	**Path 4**
0	12.06			
0.5	11.38			
1	10.64			
2	9.03		9.14	
4	5.51			
6	1.85			
8 onwards	No intersection			

TABLE IV. LOCATION ESTIMATES USING LOAD CURRENT PROFILE

Fault Resistance(Ω)	*Distance to fault along (miles)*			
	Path 1	**Path 2**	**Path 3**	**Path 4**
0	0.37			
0.5	0.71	4.5		
1	3.11	3.11		
2	11.74			12.51
4 Ω onwards	No intersection			

As shown in Tables III and IV, the estimated fault locations calculated by both current profiles do not match for any value of fault resistance. This means that the test fault case corresponds to a fault resistance for which current profiles are not available in the database.

The next step is to estimate the range within which the actual resistance might lie. To do so, the fault location estimates along path 1 are considered using both current profiles. Note that the estimated fault location using fault current profiles decreases with the increase in resistance. However, using load current profile it increases with the increase in fault resistance. Using this observation, the only possible resistance value that can result in a common location for both current profiles is in between 1Ω and 2Ω. Hence, the current profiles corresponding to fault resistance equal to 1Ω and 2Ω are used to obtain approximate current profiles. Fig. 12-13 shows the approximated current profiles correspond to fault resistance equal to 1.5 Ω. The fault location estimates using both approximate load and fault current profiles for 1.5 Ω fault resistance matches approximately at 10 miles along path 3 which is also the actual fault location.

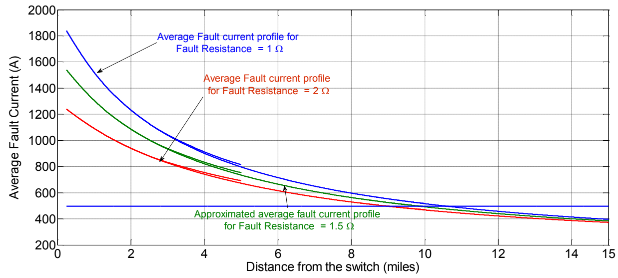

Figure 12. Estimating fault location using approximate fault current profiles for 1.5 Ω fault resistance

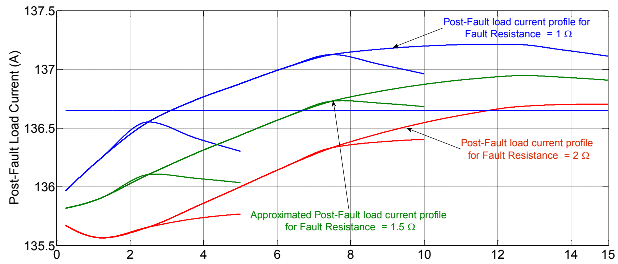

Figure 13. Estimating fault location using approximate load current profiles for 1.5 Ω fault resistance

VI. NUMERICAL EXAMPLES

The proposed hybrid current profile method is validated using the test system shown in Fig. 1. The test cases are summarized in Table V.

Due to the presence of multiple laterals and load taps, there are multiple power flow paths in the test system. Accordingly, the fault current profiles and load current profiles are developed for the circuit along each power-flow path. The effects of fault resistance are tested by using multiple cases with varied fault resistance. The test cases include both actual fault resistances for which current profiles are available, and not available in the database. The current profiles stored in the database are corresponding to a fault resistance equal to 0 Ω, 0.5 Ω, 1 Ω, 2 Ω, 4 Ω, 6 Ω, 8 Ω, and 10 Ω. The fault location is varied along each power flow path, and for each case, the estimation error is calculated.

TABLE V. SIMULATED FAULT CONDITIONS

Test Cases	*Double-Line to Ground fault*
Fault Distance	Simulated along each power flow paths in step of 0.5 miles
Fault resistance (Ω) (current profiles are available in the database)	0, 2, 4, 6
Fault resistance (Ω) (current profiles are not available in the database)	0.75,1.5,2.5, 3

A. Effect of Fault Resistance when Current Profiles are Available in the Database

In this section the effect of fault resistance on the accuracy of estimating the fault location using the proposed algorithm is evaluated. For the test cases, the current profiles corresponding to the actual fault resistance are available in the current profile database. The distribution circuit is evaluated for fault resistance equal to 0 Ω, 2 Ω, 4 Ω and 6 Ω. The fault location is varied in a step of 0.5 miles along each power-flow path and fault location is estimated for each fault scenario using the proposed algorithm.

Table VI lists the maximum and average estimation errors of proposed algorithm for all the test cases. It also gives the location or the path observing maximum error in fault location estimate. Note that, since the current profiles corresponding to actual fault resistance are available in the database, the error in the estimated fault location is not very significant. As shown in Table VI, the maximum error is reported along path 2 for all cases.

TABLE VI. EFFECT OF FAULT RESISTANCE ON FAULT LOCATION WHEN CURRENT PROFILES ARE AVAILABLE IN DATABASE

Fault Resistance(Ω)	*Maximum Error(*miles)	*Average Error(miles)*	*Location of the maximum error*
0	0.03	0.002	Along Path 2 at Bus 728
2	0.09	0.008	Along Path 2 at Bus 728
4	0.18	0.02	Along Path 2 at Bus 728
6	0.33	0.03	Along Path 2 at Bus 728

B. Effect of Fault Resistance when Current Profiles are not Available in the Database

This section evaluates the effects of fault resistance on fault location estimate when the current profiles for the actual fault resistance are not available in the database. The distribution circuit is evaluated for the simulated fault resistance equal to 0.75 Ω, 1.5 Ω, 2.5 Ω and 3 Ω. This case study is conducted to evaluate the effectiveness and accuracy of the proposed extrapolation algorithm for un-simulated fault resistance values.

The fault location is varied in a step of 0.5 miles along each power-flow path and fault location is estimated using the proposed algorithm. The test results are given in Table VII, including the maximum and average errors of fault location estimates, and the location where the maximum error in fault location is recorded. Compared Table VII with Table VI, it should be noted that the maximum error in the estimated fault location is comparatively bigger when the actual fault resistance is different from the values available in database. A maximum error of 0.97 miles is reported when the fault resistance is 2.5 Ω. However, the average error recorded in the fault location is still low and is less than 0.25 miles for each value of fault resistance under evaluation.

TABLE VII. EFFECT OF FAULT RESISTANCE ON FAULT LOCATION WHEN CURRENT PROFILES ARE NOT AVAILABLE IN DATABASE

Fault Resistance(Ω)	*Maximum Error(*miles)	*Average Error(miles)*	*Location of the maximum error*
0.75	0.92	0.23	Along Path 1 at Bus 785
1.5	0.79	0.23	Along path 2
2.5	0.97	0.23	Along path 2 at Bus 728
3	0.59	0.25	Along path 1 at Bus 725

VII. CONCLUSIONS

This paper proposes a hybrid-current profile approach for estimation of fault location in an event of a double-line-to-ground fault (DLG). The proposed method uses both fault current profile for faulted phases and during-fault load current profile for un-faulted phase to determine the fault location. The effects of fault resistances are also successfully included in the fault location algorithm.

The algorithm is tested using a distribution feeder 15 miles long, with multiple laterals and load taps. Simulation results are provided to validate the proposed algorithm for its robustness in event of DLG fault. The algorithm is tested its accuracy in the presence fault resistance. The proposed algorithm reports a maximum error of less than 0.33 miles, when current profiles for the actual fault resistance are available in the database, and 0.97 miles when current profiles for the actual fault resistance are not available and are obtained by using linear extrapolation. The average errors recorded are comparatively less, reporting 0.03 miles error in fault location when the current profiles corresponding to the actual fault resistance are available and 0.25 miles error when current profiles are obtained by approximation. Thus on an average, the proposed algorithm is successful in identifying the fault location within an acceptable accuracy.

REFERENCES

[1] R. Das, M.S. Sachdev, and T.S. Sidhu, "A Fault Locator for Radial Sub-transmission and Distribution Lines", presented at *IEEE PES Summer Meeting*, Seattle, Washington, July 2000.

[2] R.H. Salim, M. Resener, A.D. Filomena, K. Rezende Caino de Oliveira, and A. S. Bretas, "Extended Fault-Location Formulation for Power Distribution Systems", *IEEE Transactions on Power Delivery*, vol. 24, no. 2, pp. 508-516, April 2009.

[3] Z.Q. Bo, G. Waller, and M. A. Redfern, "Accurate Fault Location Technique For Distribution System Using Fault-Generated High-Frequency Transient Voltage Signals", *IEE Proceedings on Generation, Transmission and Distribution*, vol.146, no.1, pp. 73-79, January 1999.

[4] H. Nouri, C. Wang, and T. Davies, "An accurate fault location technique for distribution lines with tapped loads using wavelet transform", *IEEE Power Tech Proceedings*, Porto, Portugal, vol. 3, pp. 1-4, September 2001.

[5] J. J. Mora, G. Carrillo, and L. Perez, "Fault location in power distribution systems using ANFIS Nets and current patterns", presented at *IEEE PES Transmission and Distribution Conference and Exposition,* Latin America, Caracas, Venezuela, 2006.

[6] J. Mora-Florez, V. Barrera-Nuez, and G. Carrillo-Caicedo, "Fault location in power distribution Systems using a learning algorithm for multivariable data analysis," *IEEE Transactions on Power Delivery*, vol. 22, no. 3, pp. 1715-1721, Jul. 2007.

[7] G. C. Lampley, "Fault Detection and Location on Electrical Distribution System Case Study," presented at *IEEE Rural Electric Power Conference*, May 2002.

[8] S. Das, S. Kulkarni, N. Karnik, and S. Santoso, "Distribution fault location using short-circuit fault current profile approach", presented at *IEEE PES General Meeting,* July 2011.